

Magnetic and pulsational variability of Przybylski’s star (HD 101065)

S. Hubrig^{1*}, S. P. Järvinen¹, J. Madej², V. D. Bychkov³, I. Ilyin¹, M. Schöller⁴,
L. V. Bychkova³

¹*Leibniz-Institut für Astrophysik Potsdam (AIP), An der Sternwarte 16, 14482 Potsdam, Germany*

²*Astronomical Observatory, University of Warsaw, Al. Ujazdowskie 4, 00-478 Warszawa, Poland*

³*Special Astrophysical Observatory of the Russian Academy of Sciences (SAO), Nizhnij Arkhyz 369167, Russia*

⁴*European Southern Observatory, Karl-Schwarzschild-Str. 2, 85748 Garching, Germany*

Accepted XXX. Received YYY; in original form ZZZ

ABSTRACT

Since its discovery more than half a century ago Przybylski’s star (HD 101065) continues to excite the astronomical community by the unusual nature of its spectrum, exhibiting exotic element abundances. This star was also the first magnetic chemically peculiar A-type star for which the presence of rapid oscillations was established. Our analysis of newly acquired and historic longitudinal magnetic field measurements indicates that Przybylski’s star is also unusual with respect to its extremely slow rotation. Adopting a dipolar structure for the magnetic field and using a sine wave fit to all reported longitudinal magnetic field values over the last 43 yr, we find a probable rotation period $P_{\text{rot}} \approx 188$ yr, which however has to be considered tentative as it does not represent a unique solution and has to be verified by future observations. Additionally, based on our own spectropolarimetric material obtained with HARPS-pol, we discuss the impact of the anomalous structure of its atmosphere, in particular of the non-uniform horizontal and vertical distributions of chemical elements on the magnetic field measurements and the pulsational variability. Anomalies related to the vertical abundance stratification of Pr and Nd are for the first time used to establish the presence of a radial magnetic field gradient.

Key words: stars: individual: Przybylski’s star – stars: magnetic fields – stars: chemically peculiar – stars: rotation – stars: abundances – stars: oscillations

1 INTRODUCTION

HD 101065 was recognized first by Przybylski (1961) and became one of the most fascinating objects due to its exotic element abundances, such as a strong Fe underabundance and a large excess of almost all rare earth elements (REE). HD 101065 is generally referred to as Przybylski’s star. Using wavelength coincidence statistics, Cowley et al. (2004) suggested the presence of Pm I, Pm II, Tc I, and possibly Tc II in the spectrum of this star. HD 101065 is a main-sequence cool chemically peculiar A type star, a so-called Ap star, and belongs to the group of rapidly oscillating Ap (roAp) stars, which pulsate in high radial overtone p modes with periods in the range 6–24 min. The presence of rapid oscillation with a period of 12.14 min was detected by Kurtz & Wegner (1979).

A strong longitudinal magnetic field up to -2.5 kG was

for the first time measured in 1974 by Wolff & Hagen (1976). The average value for the longitudinal field of -2.2 kG was obtained using three measurements based on Zeeman spectra recorded on photographic plates. The random standard deviation of each field determination was estimated as 450 G. Wolff & Hagen (1976) noted that there is no evidence for a variability of the magnetic field strength over a time interval of one year.

The magnetic fields in Ap stars can be described with the oblique rotator model (Stibbs 1950). To a first approximation their fields can be modeled with a simple dipole structure with the axis of the magnetic dipole inclined to the rotation axis. To determine the rotation period in Ap stars, apart from photometric variability studies, spectropolarimetric and spectroscopic studies are widely used to monitor the variation of the longitudinal magnetic field or the magnetic field modulus, measured in magnetically resolved lines. According to Mathys (2015), Ap stars have rotation periods that span 5 to 6 orders of magnitude, from about

* E-mail: shubrig@aip.de

Table 1. Logbook of the HARPSpol observations.

HJD	Date	<i>S/N</i>
2457179.4993	2015-06-05	314
2457555.6030	2016-06-16	377
2457908.5970	2017-06-04	232
2457911.6047	2017-06-07	351

0.5 d to about 300 years or even longer, and as of today, the long-period tail of the distribution of the rotation periods of Ap stars is populated almost exclusively by stars that show magnetically resolved lines. Magnetically split components are usually observed in stars with a magnetic field modulus down to 2.2 kG (Mathys et al. 1997). Since the spectrum of HD 101065 exhibits rather narrow spectral lines with $v \sin i = 3.5 \pm 0.5 \text{ km s}^{-1}$ (Cowley et al. 2000), it was possible to measure a weak magnetic broadening corresponding to 2.3 kG obtained from partially resolved Gd II and Sm II lines (Cowley et al. 2000). According to Mkrtichian et al. (2008), HD 101065 appears to be a prime candidate to possess a very long rotation period.

To study the periodicity of the magnetic variability of this star we carried out over the last three years high-resolution spectropolarimetric observations using the High Accuracy Radial velocity Planet Searcher polarimeter (HARPSpol; Snik et al. 2008) attached to ESO’s 3.6 m telescope (La Silla, Chile). We complemented the measured longitudinal magnetic field strengths with magnetic measurements from the literature to characterize the field variation curve. Additionally, since magnetic Ap stars and, in particular, roAp stars frequently display non-uniform horizontal and vertical distributions of chemical elements, we investigate the possible impact of such atmospheric properties on the measured magnetic field strength and the pulsational characteristics.

2 OBSERVATIONS AND DATA REDUCTION

HARPSpol observations using the circular polarization analyzer were obtained on the nights of 2015 June 5, 2016 June 16, and 2017 June 4 and 7. The recorded spectra cover the 3780–6910 Å wavelength range with a small gap between 5259 and 5337 Å at a spectral resolution of $R \approx 115000$. We observed the star with a sequence of two sub-exposures in the first three occasions and of four sub-exposures during the last epoch, obtained rotating the quarter-wave retarder plate by 90° after each sub-exposure. The reduction and calibration of these spectra was performed using the HARPS data reduction software available on La Silla. The normalization of the spectra to the continuum level was described in detail by Hubrig et al. (2013). The dates of observations and the achieved signal-to-noise ratios in the Stokes *I* spectra are presented in Table 1.

3 MAGNETIC FIELD ANALYSIS

3.1 Measurements using the least-squares deconvolution technique

To measure the longitudinal magnetic field, we employed the least-squares deconvolution (LSD) technique, allowing us to achieve a much higher signal-to-noise ratio (*S/N*) in the LSD spectra. LSD combines line profiles (assumed to be identical) centred on the position of the individual lines and scaled according to the line strength and sensitivity to a magnetic field (i.e. line wavelength and Landé factor). The details of this technique and of the calculation of the Stokes *I* and *V* parameters can be found in the work of Donati et al. (1997).

Magnetic Ap stars frequently display non-uniform horizontal and vertical distributions of chemical elements. Some elements show preferential surface concentration close to the magnetic poles, while other elements are concentrated closer to the magnetic equator regions. Thus, the lines of different elements with different abundance distributions across the stellar surface sample the magnetic field in a different manner. Combining lines belonging to different elements altogether, as is frequently done with the LSD technique, may lead to dilution of the magnetic signal or even to its (partial) cancellation, if enhancements of different elements occur in regions of opposite magnetic polarity.

To investigate the possible impact of such a horizontal non-uniformity, we decided to measure the magnetic field using eight different line masks: one mask Fe, which includes the least blended iron lines, five individual masks for the best identified lines belonging to lanthanides, such as La, Ce, Pr, Nd, and Sm, one mask REE that combines all individual masks for the lanthanides, and one mask All that combines the masks Fe and REE. These eight line masks were constructed using the Vienna Atomic Line Database (VALD3; Kupka et al. 2011) and the stellar parameters $T_{\text{eff}} = 6400 \text{ K}$ and $\log g = 4.2$ reported for HD 101065 in the study by Shulyak et al. (2010). The LSD Stokes *I* and *V* spectra, calculated for the eight line masks, were used for the measurement of the longitudinal magnetic field through the first order moment of the Stokes *V* profile (e.g. Mathys 1989).

In Table 2 we present the number of lines in each line mask, the average Landé factors and the measured longitudinal magnetic field values for the observations obtained between 2015 and 2017. In all cases the false alarm probability (FAP) is less than 10^{-15} . According to the convention of Donati et al. (1992), a Zeeman profile with $\text{FAP} \leq 10^{-5}$ is considered as a definite detection, $10^{-5} < \text{FAP} < 10^{-3}$ as a marginal detection, and $\text{FAP} > 10^{-3}$ as a non-detection.

The LSD Stokes *I*, *V*, and diagnostic null (*N*) spectra for all line masks are presented in Fig. 1. The diagnostic *N* profiles are usually used to identify spurious polarization signatures. They are calculated by combining the subexposures in such a way that the polarization cancels out. The essentially flat null spectra presented in Fig. 1 indicate the absence of spurious contributions to our measurements.

3.2 Horizontal inhomogeneous element distribution

The LSD Stokes *I* spectra in the lower panels of Fig. 1 clearly demonstrate abundance excesses of REE and a deficiency of

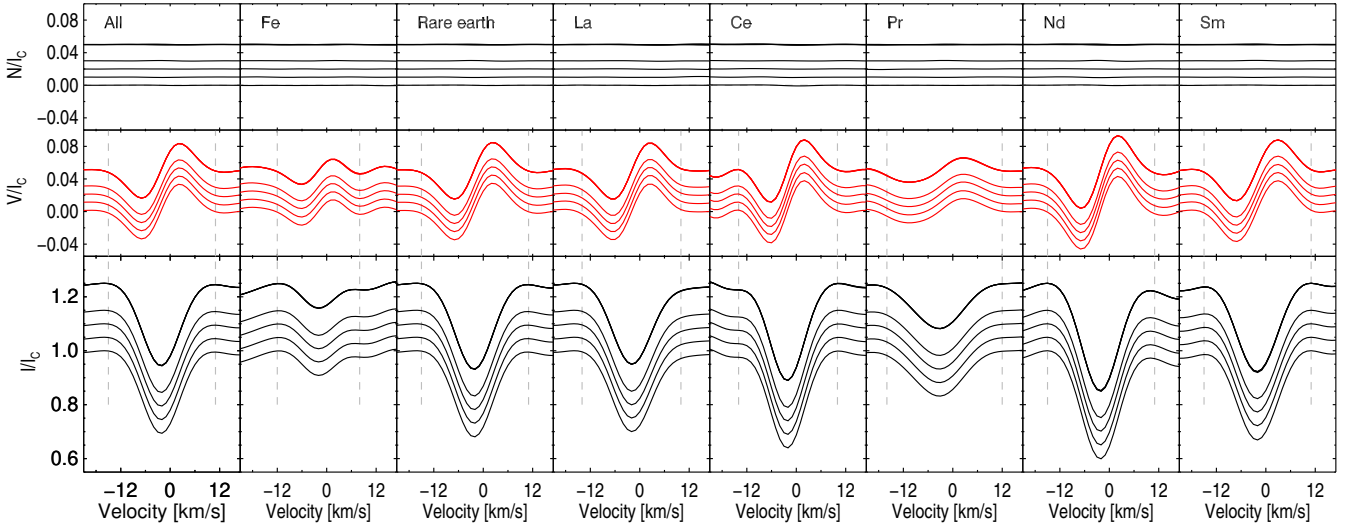


Figure 1. LSD Stokes I (bottom), Stokes V (middle), and diagnostic null (N) spectra (top) obtained for HD 101065 on four nights between 2015 and 2017. The LSD spectra were calculated using eight different line lists, indicated in each panel. For each panel, spectra for 2015 June 5, 2016 June 16, 2017 June 4, and 2017 June 7 are shown from bottom to top; the last three are shifted upwards for better visibility. The LSD Stokes I , Stokes V , and diagnostic null (N) spectra at the top show all four spectra overplotted.

iron, already mentioned in previous works (e.g. Cowley et al. 2000). Among the REE, the neodymium and cerium lines are the strongest in the spectrum of HD 101065, whereas the praseodymium lines appear rather weak. The LSD Stokes V spectra show the presence of clear Zeeman features corresponding to a longitudinal magnetic field of negative polarity. The field strengths for each line mask measured on the four epochs over the three years appear to be constant within uncertainties. On the other hand, the measurements using individual masks with lines corresponding to different elements reveal distinct differences in the field strengths, with the lowest field value obtained for cerium, $\langle B_z \rangle \approx -620$ G, and the strongest field value, $\langle B_z \rangle \approx -860$ G, for neodymium. This suggests that the neodymium lines may form in spots that are close to the magnetic pole, while cerium lines form at some distance from the magnetic pole.

Significant differences in the magnetic field strengths measured using spectral lines belonging to different elements were already mentioned in the past by Hubrig et al. (2004b) who used spectropolarimetric observations of several Ap stars with the FOCAL Reducer low dispersion Spectrograph (FORS1; Appenzeller et al. 1998) mounted on the 8 m Antu telescope of the VLT. The authors reported that the magnetic field strength measured in Balmer lines can be by up to 500 G lower compared with measurements where metal lines are included. The detected differences between measurements carried out using lines of different elements can most likely be ascribed to significant inhomogeneous distributions of these elements in both horizontal and vertical directions, indicating a very peculiar atmospheric structure in this star.

3.3 Vertical stratification of Pr and Nd

Most of the studied roAp stars show a REE anomaly, i.e. abundances derived from REE lines of different ionization stages show differences of up to a few dex (e.g. Cowley et al.

2000; Ryabchikova et al. 2004). It is generally assumed that a strong magnetic field suppresses convection and provides a stable environment where radiative levitation of some elements occurs. This radiative diffusion mechanism leads to a stratified atmosphere where the abundance distribution in vertical direction can for simplicity be approximated by a step function with a different element abundance in the higher atmospheric layer compared to that in the deeper layer (e.g. Shulyak et al. 2009).

The REE anomaly in HD 101065 was for the first time discovered by Cowley et al. (2000) and it was suggested that due to the influence of radiative diffusion, REE are accumulated in the upper atmospheric layers. According to Shulyak et al. (2010), due to the heavy blending of REE lines in the spectrum of this star, their stratification analysis is highly complicated. The authors emphasize that similar to the hotter roAp star HD 24712 with a strong accumulation of REE in the upper atmosphere producing a characteristic inverse temperature gradient, one would expect the same mechanism to operate in the atmosphere of HD 101065. In an attempt to construct an empirical self-consistent model atmosphere for HD 24712, where the stratification of chemical elements is derived directly from the observed spectra and then treated in a model atmosphere code, Shulyak et al. (2009) report that the strong overabundance of Pr and Nd leads to the appearance of an inverse temperature gradient with a maximum temperature increase of up to 600–800 K compared to a homogeneous abundance model. The spectra of many roAp stars also show a strong core-wing anomaly in the hydrogen lines, particularly the $H\alpha$ line (e.g. Cowley et al. 2001). This anomaly is usually explained by non-standard temperature gradients.

The anomalous structure of the atmosphere of HD 101065 is also evident in our observations. As an example, we present in Fig. 2 the LSD Stokes I , V , and diagnostic null (N) spectra for observations in 2016 obtained with the highest S/N using four masks containing lines belonging to

Table 2. Longitudinal magnetic field strengths measured at four different observing epochs using the LSD technique for the eight different line masks. In Columns 2 and 3 we present the number of lines in the individual line masks and the average Landé factor. For each line list, the four rows in the last column correspond to the measurements obtained on the observing dates 2015 June 5, 2016 June 16, 2017 June 4, and 2017 June 7, respectively. In all cases the false alarm probability is less than 10^{-15} .

Line mask	# of lines	Landé Factor	$\langle B_z \rangle$ (G)
All	417	1.160	-732 ± 20 -734 ± 19 -738 ± 20 -735 ± 19
Fe	23	1.211	-722 ± 62 -737 ± 63 -708 ± 62 -720 ± 61
REE	394	1.157	-751 ± 19 -752 ± 19 -757 ± 19 -754 ± 19
La	47	1.072	-652 ± 52 -658 ± 51 -668 ± 53 -660 ± 51
Ce	57	1.059	-609 ± 78 -616 ± 80 -626 ± 75 -620 ± 76
Pr	84	1.116	-636 ± 68 -636 ± 71 -668 ± 71 -642 ± 72
Nd	145	1.134	-856 ± 32 -863 ± 31 -865 ± 32 -861 ± 30
Sm	61	1.424	-713 ± 31 -709 ± 32 -717 ± 31 -714 ± 33

the first and second ionization stages of Pr and Nd. These elements have a larger number of identified lines compared to other REE and thus are best suited for our analysis. The visual inspection of the LSD Stokes I profiles shows that Pr and Nd lines in the second ionization stage appear stronger than Pr and Nd lines in the first ionization stage. According to Mashonkina et al. (2005, 2009), the line formation of Pr and Nd can strongly deviate from the local thermodynamic equilibrium (LTE) and the doubly ionized lines of these elements are unusually strong due to combined effects of vertical stratification and departures from LTE.

It is noteworthy that REE anomalies related to vertical abundance stratification can be used to establish the presence of the magnetic field gradient in the stellar atmospheres. Using the line mask for the Nd II lines we measure in the spectra obtained on 2016 June 16 a longitudinal mag-

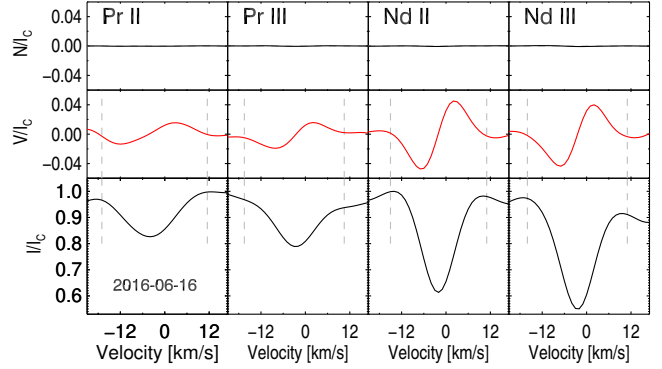


Figure 2. As Fig. 1 but using the Pr II, Pr III, Nd II, and Nd III lines in the spectra obtained on 2016 June 16.

netic field $\langle B_z \rangle = -970 \pm 38$ G whereas using the line mask for the Nd III lines we obtain $\langle B_z \rangle = -667 \pm 32$ G. The effect of the magnetic field gradient is less noticeable for Pr, where we measure for the Pr II lines $\langle B_z \rangle = -689 \pm 102$ G, and $\langle B_z \rangle = -588 \pm 80$ G using the line mask for the Pr III lines. Identical results on the presence and strength of a magnetic field gradient were also obtained using the lines belonging to the REE in the individual observations acquired in 2015 and 2017. To increase the accuracy of our measurements, we also calculated mean HARPSpol spectra representing the average polarimetric spectra over all three years and remeasured the magnetic field using the Pr and Nd lines of different ionization stages. We obtain $\langle B_z \rangle = -969 \pm 17$ G using the Nd II lines and $\langle B_z \rangle = -663 \pm 18$ G using the Nd III lines, whereas using the line mask for the Pr II lines we measure $\langle B_z \rangle = -690 \pm 35$ G and $\langle B_z \rangle = -596 \pm 28$ G using the Pr III lines.

The large difference in the magnetic field strengths measured on the Nd lines of different ionization stages with the stronger magnetic field detected in the Nd II lines and a weaker magnetic field in the Nd III lines is highly intriguing and unexpected. For a non-peculiar A-type star, we would expect lines of Nd and Pr of the second ionization stage to be formed lower in the atmosphere than lines of Nd and Pr of the first ionization stage. Assuming a dipole configuration of the magnetic field, we would then expect to measure a stronger magnetic field in the lines of Nd III and Pr III. However, assuming a normal atmospheric structure, our measurements show a significant decrease of the magnetic field strength with atmospheric depth. The measured inverse magnetic field gradient can most probably be explained by non-standard temperature gradients in the atmospheres of roAp stars.

In line with these results, Nesvacil et al. (2004) found a significant decrease of the magnetic field strength, of the order of a few hundred Gauss, with atmospheric depth in a few Ap stars using measurements of the mean magnetic field modulus from spectral lines resolved into magnetically split components lying on different sides of the Balmer jump. One star in their sample, the roAp star 33 Lib, showed the largest difference (up to 6σ) in the mean magnetic field modulus measured at different atmospheric depths. However, estimations of the optical depth for the analyzed spectral lines in that work were carried out using atmosphere models for

normal non-magnetic stars and certainly do not correspond to realistic optical depths, which are expected to be different in roAp stars due to the appearance of an inverse temperature gradient. Indeed, Kurtz et al. (2004) studied the atmospheric depth dependence of pulsations in 33 Lib as a function of atmospheric depth and suggested that Nd II and Nd III lines form on opposite sides of a pulsation node with Nd III above and Nd II below the node. Also the work of Mkrtichian et al. (2003) on radial velocity variations in these stars indicates that Nd III lines are formed significantly higher in the stellar atmosphere than Nd II. Since HD 101065 is a typical roAp star, we expect neodymium stratification with Nd III lines formed in the upper layer of this star. Thus, the stronger magnetic field measured using the Nd II lines corresponds to a larger atmospheric depth as expected for a dipole configuration of the magnetic field.

In view of the extremely abnormal chemical composition of the atmospheres and the presence of strong magnetic fields, the calculation of the element abundance distribution with respect to the optical depths in roAps is a very complex process requiring the fitting of spectroscopic, photometric, and magnetic data. The vertical stratification of the chemical elements was modeled in previous studies of roAp stars in a simplified way, assuming a simple step-like profile of the distribution of elements. However, in realistic self-consistent atmospheric models the stratification and abundance analysis should be linked to the model atmosphere calculation. Obviously, significant improvements in the physics of atmospheric models and in opacity sources, also taking into account realistic magnetic-field configurations, are urgently needed.

3.4 Application of the moment technique

We also analysed the HARPS spectropolarimetric material with a different approach for the measurements of the magnetic field, namely the moment technique developed by Mathys (1991, 1995). This technique allows us not only to determine the mean longitudinal magnetic field, but also to prove the presence of the crossover effect and measure the quadratic magnetic field. This information cannot be obtained from the LSD technique.

The mean quadratic magnetic field is derived through the application of the moment technique, described e.g. by Mathys & Hubrig (2006). It is determined from the study of the second-order moments of the line profiles recorded in unpolarized light (that is, in the Stokes parameter I):

$$\langle B_q \rangle = (\langle B^2 \rangle + \langle B_z^2 \rangle)^{1/2}, \quad (1)$$

where $\langle B^2 \rangle$ is the mean square magnetic field modulus, i.e. the average over the stellar disc of the square of the modulus of the magnetic field vector, weighted by the local emergent line intensity, while $\langle B_z^2 \rangle$ is the mean square longitudinal magnetic field, i.e. the average over the stellar disc of the square of the line-of-sight component of the magnetic vector, weighted by the local emergent line intensity. The crossover effect can be measured by the second order moment about their centre of the profiles of spectral lines recorded in the Stokes parameter V . It was for the first time shown by Mathys (1995) that it is possible to derive from the measurements a quantity called the mean asymmetry of

Table 3. Historic magnetic field measurements. In the first column we list the heliocentric Julian date at the time of observation, followed by the longitudinal magnetic field value. The references to the related studies are presented in the last column.

HJD	$\langle B_z \rangle$ (G)	Reference
2442386.22	-1567 ± 210	Wolff & Hagen (1976)
2448782.54	-1408 ± 50	Cowley & Mathys (1998)
2452383.20	-1041 ± 53	Hubrig et al. (2004b)
2452701.25	-1004 ± 75	
2454209.76	-1107 ± 19	Hubrig, unpublished
2454222.60	-1071 ± 19	
2454233.49	-1046 ± 20	
2454247.47	-1086 ± 20	
2454254.57	-1051 ± 20	
2454272.53	-1036 ± 19	
2454281.48	-1012 ± 20	
2454297.52	-1024 ± 20	
2454306.54	-932 ± 26	

the longitudinal magnetic field, which is the first moment of the component of the magnetic field along the line of sight, about the plane defined by the line of sight and the stellar rotation axis.

We employed in the analysis the same 23 least blended Fe I lines as those used in the LSD method. In agreement with the LSD results, our measurements of HARPSpol spectra reveal the longitudinal magnetic field $\langle B_z \rangle = -757 \pm 63$ G at a significance level of 12σ . We do not detect any significant crossover on the four observing epochs, as expected for stars with very long rotation periods, but we detect a mean quadratic magnetic field of the order of 1.6 ± 0.3 kG. No significant longitudinal fields were determined from the diagnostic null spectra.

4 MAGNETIC FIELD VARIABILITY

The fact that the longitudinal magnetic field strengths for each line mask measured on four epochs over the last three years are constant within the measurement uncertainties indicates that the rotation period of HD 101065 is long. In Table 3 we list all available longitudinal magnetic field measurements published in the literature. We also present a number of FORS1 longitudinal magnetic field measurements that we did not publish earlier. The dispersion of the longitudinal magnetic field measurements obtained with FORS1 in spectropolarimetric mode attached to one 8 m telescope of the VLT can likely be explained by the rather short exposure time of each observation consisting of a sequence of eight subexposures taken at two different position angles of the retarder waveplate, $+45^\circ$ and -45° (e.g. Hubrig et al. 2004a), and of a duration of only 65 s. The duration of the full sequence of about 10 min is less than the length of the pulsation period of HD 101065 of 12.4 min. Hence an impact of pulsational variability on our FORS1 measurements cannot be excluded. From the theoretical considerations presented by Hubrig et al. (2004b) follows that a pulsationally-modulated variation of the order of 100 G may

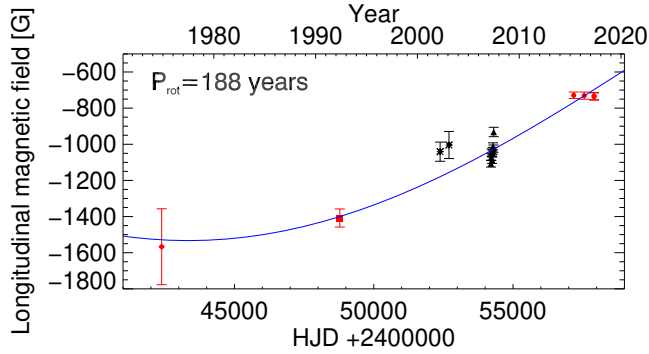


Figure 3. Variation of the longitudinal magnetic field values $\langle B_z \rangle$ for HD 101065 as a function of HJD between 1974 and 2017. The photographic measurements by [Wolff & Hagen \(1976\)](#) and the high-resolution CCD measurements are highlighted in red (in the online version), whereas the low-resolution FORS1/2 measurements are indicated in black color. Vertical error bars show the measurement accuracies.

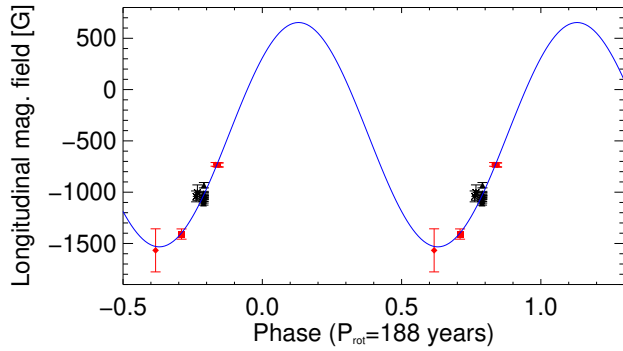


Figure 4. The longitudinal magnetic field values $\langle B_z \rangle$ for HD 101065 measured over 43 yr and phased with the period of 188 yr.

exist in the outer atmospheric layers of roAp stars with kG magnetic fields. We note that due to a lack of good atomic data used for the calculation of the Landé factors in the study of [Wolff & Hagen \(1976\)](#), we adopted the revised longitudinal magnetic field value $\langle B_z \rangle = -1567 \pm 210$ G reported by [Mkrtichian et al. \(2008\)](#). These measurements including our most recent HARPSpol measurements clearly indicate a gradual decrease of the longitudinal magnetic field strength (see also e.g. [Mkrtichian et al. 2008](#)).

In Fig. 3 we plot the longitudinal magnetic field values for HD 101065 as a function of HJD between 1974 and 2017. Adopting a dipolar structure for the magnetic field and using a sine wave fit to all reported field values, a minimum χ^2 solution of 4.6 utilizing the Levenberg–Marquardt method ([Press et al. 1992](#)) was found for a probable rotation period of $P_{\text{rot}} \approx 188$ yr. In Fig. 4 we present the observed trend in the magnetic field measurements over 43 yr together with the full sine wave computed for this period. Obviously, since only 23% of the period of about 188 yr is covered by the magnetic field measurements, this very long period should be considered tentative and has to be verified by additional observations in the next tens of years.

Table 4. Variability of the LSD Stokes I spectral profiles calculated for each line mask for the sequences of HARPS sub-exposures obtained on time scales in the range of 30–90 min. For each line list, the four rows correspond from top to bottom to the observing dates 2015 June 5, 2016 June 16, 2017 June 4, and 2017 June 7, respectively. The line profile variability in the line cores and in the line wings in % of the normalized flux is presented in Columns 2 and 3, whereas the RV shifts in km s^{-1} are listed in Column 4. For the only observation with four subexposures obtained in 2017 June 7 we give the variability ranges.

Line mask	Core Variability (%)	Wing Variability (%)	RV (km s^{-1})
All	0.191 0.201 0.190 0.177–0.200	0.616 0.281 0.879 0.161–1.150	−0.15 −0.07 −0.21 −0.03–0.27
Fe	0.157 0.171 0.004 0.049–0.085	0.699 0.197 0.357 0.250–0.405	−0.12 −0.04 −0.21 −0.08–−0.28
REE	0.192 0.204 0.200 0.181–0.203	0.684 0.306 0.919 0.171–1.238	−0.14 −0.07 −0.21 −0.03–−0.28
La	0.172 0.239 0.135 0.120–0.197	1.435 0.599 1.093 0.268–1.334	−0.09 −0.07 −0.20 −0.02–−0.24
Ce	0.397 0.440 0.468 0.373–0.395	0.471 0.261 0.778 0.183–0.869	−0.22 −0.10 −0.20 −0.03–−0.24
Pr	0.126 0.061 0.104 0.015–0.096	0.260 0.121 0.394 0.066–0.541	0.02 0.03 −0.21 −0.30–0.02
Nd	0.309 0.292 0.297 0.245–0.298	0.689 0.282 1.120 0.227–1.514	−0.13 −0.06 −0.20 −0.03–−0.27
Sm	0.087 0.056 0.145 0.060–0.101	1.081 0.546 1.201 0.282–1.484	−0.23 −0.13 −0.27 −0.04–−0.36

5 PULSATONAL VARIABILITY

The roAp stars were the first stars for which high-overtone p-mode pulsations were detected. Previous pulsational studies using high-resolution spectroscopic time series also showed that pulsation radial velocity (RV) amplitudes are different for different elements, with the highest amplitudes detected in REE (e.g. [Elkin et al. 2010, 2015](#)). HD 101065 is reported to show one of the highest photometric pulsation amplitudes ([Kurtz et al. 2006](#)) and rather high pulsation RV amplitudes of almost 0.9 km s^{-1} for lines of Pr III and up to about 0.2 km s^{-1} for Ce II lines ([Elkin et al. 2015](#)).

HARPSpol observations are usually split into either two

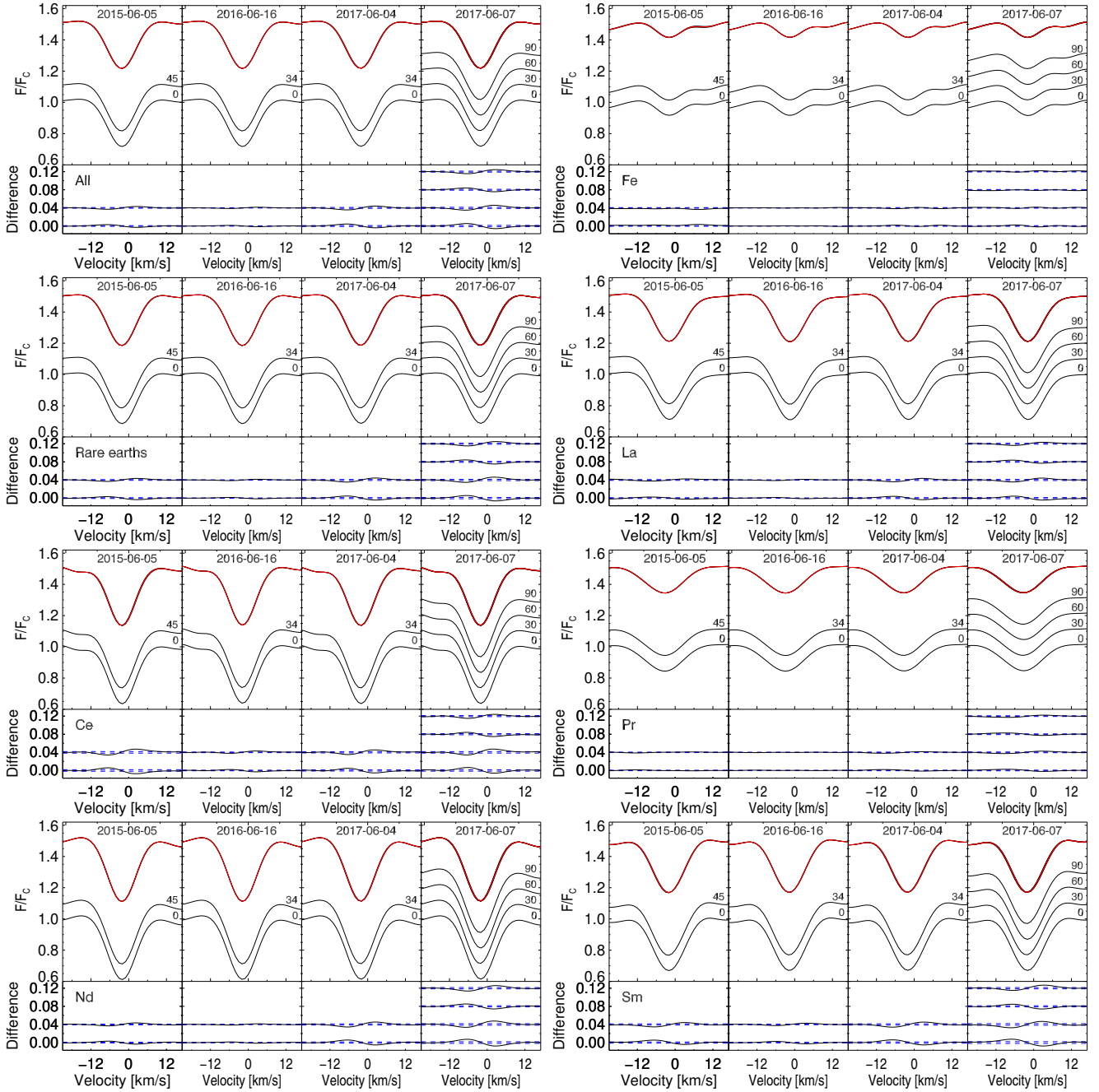


Figure 5. The LSD line profiles calculated for the line masks All, Fe, REE, and several individual REE (La, Ce, Pr, Nd, and Sm). *Top panels:* Comparison of the LSD Stokes I profiles computed for the individual subexposures. The individual profiles are shifted vertically for better visibility. The upper row shows overplotted profiles together with the average profile (red in the online version). The time difference in minutes between the individual and the first subexposures is given next to the line profiles. *Bottom panels:* Differences between Stokes I profiles computed for the individual subexposures and the average Stokes I profile. The dashed lines indicate the standard deviation limits.

or four subexposures and allow us to study any changes in the line profile shape or RV shifts on the time scales corresponding to the duration of the individual subexposures, which is of the order of 30–45 min. We note, however, that since this duration is by a factor of 2.5–3.7 longer than the pulsation period of HD 101065, we expect that any pulsational variability is smeared over the length of our subexposures. We should also keep in mind that the accuracy of the continuum normalization of our spectra is limited by photon

noise, which is larger for the subexposures compared with the signal-to-noise ratios of the final combined spectra presented in Table 1. Therefore, in the following, we consider any changes detected at a level of 1% or less as due to instrumental or reduction effects. A comparison of the LSD Stokes I profiles computed for the individual subexposures obtained on each observing night from 2015 to 2017 for all eight line masks is displayed in Fig. 5. The presence of very small changes in the LSD Stokes I line profiles is discovered

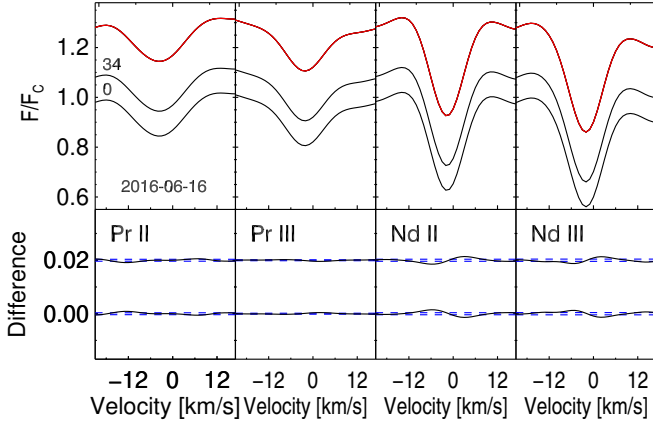


Figure 6. As Fig. 5 but using line lists for Pr II, Pr III, Nd II, and Nd III compiled for observations obtained on 2016 June 16.

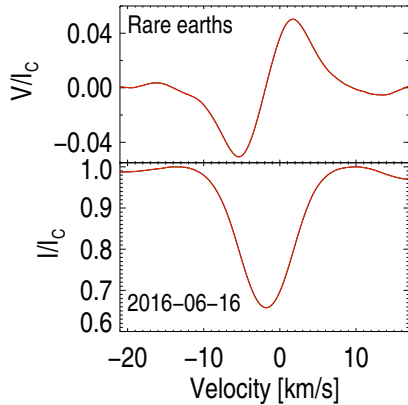


Figure 7. LSD Stokes V and I profiles calculated for the REE line list. The profiles calculated without taking into account pulsational RV shifts between two subexposures are presented by the red color (in the online version) whereas profiles corrected for the RV shift are presented in black color. They are virtually indistinguishable.

in plots constructed for the line masks All, and rare earth elements. In Table 4 we present our measurements of the LSD line profile variability for each observing epoch and all line masks. The largest variability in the line cores is detected in the cerium lines, up to 0.47% of the normalized flux, while the strongest variability in the line wings up to 1.48% and the largest RV shift up to 0.36 km s^{-1} are measured for samarium lines.

As discussed in Sect. 3.3, the line formation depth of the Pr and Nd lines in the second ionization stage is different compared with that of the Pr and Nd lines in the first ionization stage, i.e. the Pr III and Nd III lines are expected to be formed in the upper atmospheric layers. In Fig. 6 we present LSD profiles calculated separately for Pr and Nd in different ionization stages. No obvious difference between the different Pr and Nd ions is indicated in our data, probably due to the long exposure times of 34 min for our subexposures, which exceeds the pulsation period by a factor of 2.8. The variability of the line profiles belonging to Pr II and Pr III is only of the order of 0.1% of the normalized continuum.

Pulsations are also known to have an impact on the

analysis of the presence of a magnetic field and its strength by introducing line profile shifts in radial velocity and shape changes between subexposures (e.g. Hubrig et al. 2011; Järvinen et al. 2017). Especially in the case where the duration of the subexposures is comparable to the length of the pulsation period, the diagnostic null spectra calculated with the purpose to diagnose spurious polarization, usually do not appear flat. Since our subexposure duration of the order of 30–45 min is much longer than the pulsation period of HD 101065, we expect that pulsational signatures in the null spectra are substantially smoothed out. Indeed, as is shown in Fig. 1, only very tiny, hardly recognizable features are present in the null spectra calculated for the REE. The amplitude of these features is only of the order of 0.1% of the normalized flux.

To test the impact of the pulsational variability on our analysis of the magnetic field strength, the magnetic field measurements were carried out using the left-hand-polarized and right-hand-polarized spectra for each subexposure separately, as was already done in previous studies of pulsating stars by e.g. Hubrig et al. (2011) and Järvinen et al. (2017). The corresponding LSD Stokes V and I profiles calculated for the REE line list using the observations obtained in 2016 are presented in Fig. 7. No significant change in the magnetic field strength was detected in this test, suggesting that our HARPSpol magnetic field measurements are not affected by the presence of pulsations. The measurements using the line profiles corrected for the RV pulsational shift show an increase of the strength of the longitudinal magnetic field by just 21 G, which is of the order of the measurement uncertainties of 19 G. To summarize, no impact of pulsational variability is detected in our HARPSpol data.

6 DISCUSSION

Our new spectropolarimetric observations of the magnetic roAp star HD 101065 with HARPSpol over the last three years do not indicate any field strength variability within the measurement uncertainties. Using our measurements along with all available longitudinal magnetic field measurements presented in the literature and adopting a dipolar structure of the magnetic field, we estimate the probable length of the rotation period $P_{\text{rot}} \approx 188 \text{ yr}$. This result is certainly subject to the poor sampling of this period. Our estimation of a 188 yr period should thus not be considered as a unique solution, given the time coverage of the longitudinal magnetic field measurements of 43 yr, which represents a lower limit on the true rotation period of HD 101065.

Longitudinal magnetic field measurements using individual masks with lines corresponding to different elements reveal distinct differences in the field strengths, which can most likely be ascribed to inhomogeneous distributions of these elements in both the horizontal and vertical directions. The lowest longitudinal magnetic field value was obtained for cerium ($\langle B_z \rangle \approx -620 \text{ G}$) and the strongest longitudinal magnetic field value ($\langle B_z \rangle \approx -860 \text{ G}$) for neodymium, indicating that neodymium lines may form in spots that are close to the magnetic pole while cerium lines form at some distance from the magnetic pole. Among the studied elements, Nd and Ce lines are the strongest in the spectrum of HD 101065, whereas Fe and Pr lines appear rather weak.

Longitudinal magnetic field measurements using Nd lines of different ionization stages reveal the presence of a rather strong magnetic field gradient of the order of 300 G. Using the line mask for the Nd II lines we measure a longitudinal magnetic field $\langle B_z \rangle = -969 \pm 17$ G, whereas using the line mask for the Nd III lines we obtain $\langle B_z \rangle = -663 \pm 18$ G. The effect of the magnetic field gradient is less noticeable in the measurements using the Pr lines. Since HD 101065's atmosphere has an extremely abnormal chemical composition, similar to a few other roAp stars (e.g. Shulyak et al. 2010 and references therein), we expect the presence of neodymium stratification, with the Nd III lines formed in the upper atmospheric layer. Thus, the stronger magnetic field measured using the Nd II lines corresponds to a larger atmospheric depth as expected for a dipole configuration of the magnetic field.

Spectropolarimetric monitoring of HD 101065 in the next tens of years is also important for another reason. In view of the recent work of Mathys (2017), who demonstrated that a number of Ap stars with long periods exhibit anharmonicities in their magnetic phase curves, long rotation periods should be regarded with caution, as they are the result of an extrapolation based on the assumption that the longitudinal magnetic field variation curve does not significantly depart from a sinusoid. Apart from monitoring the strength of the longitudinal magnetic field of HD 101065 using circularly polarised spectra, a useful approach to establish the presence of an extremely slow rotation could be to measure broad-band linear polarisation, which is caused by different saturation of the π and σ components of a spectral line in the presence of a magnetic field. This differential effect is qualitatively similar for all lines, so that in broad-band observations the contributions of all lines add up. A model for the interpretation of such observations was developed by Landolfi et al. (1993).

According to Mathys (2015), there exist strong indications that the longest periods of Ap stars must reach about 300 yr, and even longer, up to 1000 yr. A rotation period of about 35462.5 d (~ 97 yr) was suggested by Bychkov et al. (2016) for the Ap star γ Equ (=HD 201601). Also the observations of broad-band linear polarization by Leroy et al. (1994) over about three years indicated that the rotation period of γ Equ is longer than 70 yr. Six other Ap stars were suggested to possess a rotation period longer than 10 yr. Metlova et al. (2014) showed that a rotation period of 7961.8 d (~ 22 yr) is consistent with all available photometric and spectropolarimetric observations of GY And (=HD 9996). Magnetic field monitoring of HD 965 by Romanyuk et al. (2015) indicated a rotation period of about 13 yr, while the inclusion of all available longitudinal magnetic field values in the period search suggested a period of about 17 yr (Bychkov et al. 2018, in preparation). As reported by Hubrig et al. (2002), HD 965 discloses a very similar spectral appearance to HD 101065, showing a very complex spectrum rich with lines of lanthanides. Mathys (2017) combined for 33 Lib (=HD 137949) all available longitudinal magnetic field measurements from the work of Mathys et al. (1997) and Romanyuk et al. (2014), reporting that a peak standing out rather clearly in the periodogram corresponds to a period of 5195 d (~ 14 yr). Two more Ap stars, HD 110066 and HD 41403, were reported to have long rotation periods, but the spectropolarimetric ob-

servations have very incomplete phase coverage. Using spectrophotometric observations, Adelman (1981) suggested for HD 110066 a period of about 13.5 yr. The rotation period of HD 41403 of ~ 13 yr (Bychkov et al. 2018, in preparation) is based on the work of Kudryavtsev et al. (2006). A detailed discussion of the longitudinal magnetic field measurements and the phase curves for the stars HD 201601, HD 965, HD 9996, HD 137949, and HD 110066 is presented in the work of Mathys (2017). This work also confirms the previous result of the study of Wolff (1975) that the properties of stars (chemical composition, magnetic field strength, etc.) with long periods are similar to those of Ap stars with shorter periods.

The processes playing a role in achieving the slow rotation of magnetic Ap stars are not identified yet. It is generally assumed that Ap stars are slow rotators because of magnetic braking and that most of the angular momentum is lost in the pre-main-sequence phase. Using accurate Hipparcos parallaxes for magnetic Ap stars with masses below $3M_{\odot}$, Hubrig et al. (2000a, 2007) showed that magnetic stars are concentrated towards the centre of the main-sequence band, whereas normal A stars occupy the whole width of the main sequence, without a gap. According to these results, there must exist progenitors of Ap stars in the form of normal A stars, which probably rotate slowly. It is conceivable that the Ap progenitors contain a strong field in their interior, which only appears at the surface at some evolutionary stage (e.g. Braithwaite & Nordlund 2006). A study of projected rotational velocities in young and old A stars involving a sample of 160 A-type stars with very accurate Hipparcos parallaxes did not reveal any statistically significant difference between the $v \sin i$ distributions (Hubrig et al. 2000b). The obtained results were also fully compatible with conservation of angular momentum. It is quite possible that the sample of 160 A-type stars was not representative enough for such a study and that most of the angular momentum is indeed lost in the pre-main-sequence phase, where the magnetic field responsible for braking the pre-main-sequence star's rotation is buried under the surface of the star - allowing it to rotate slowly while staying chemically normal - and appears at the surface again after the star has completed a part of its life on the main sequence.

The magnetic pre-main-sequence Herbig Ae/Be stars are frequently considered as progenitors of magnetic Ap/Bp stars as their incidence of $\sim 7\%$ is similar to that in magnetic Ap/Bp stars (Alecian et al. 2017). Magnetic fields in Herbig stars might be fossils of the early star formation epoch, in which the magnetic field of the parental magnetized core was compressed into the innermost regions of the accretion disks (e.g. Banerjee & Pudritz 2006). On the other hand, Cauley & Johns-Krull (2014) studied the He I $\lambda 10830$ morphology in a sample of 56 Herbig Ae/Be stars and suggested that Herbig Be stars do not accrete material from their inner disks in the same manner as classical T Tauri stars, which accrete material via magnetospheric accretion. Only late type Herbig Be and Herbig Ae stars show evidence for magnetospheric accretion. In magnetospheric accretion models the disk material is channeled from the disk's inner edge onto the star along the magnetic field lines implying that magnetic fields do exist on the surface of late type Herbig Be and Herbig Ae stars. Therefore, the low incidence of magnetic fields in these stars reported by Alecian et al. (2017)

is difficult to understand, but can probably be explained by the weakness of their magnetic fields (Hubrig et al. 2015). Obviously, explanations for the magnetic field origin and magnetic field evolution from the PMS stage to the end of the main-sequence life can be made only through careful consolidation of magneto-hydrodynamic theory and observations.

In conclusion, the presence of a very long rotation period in HD 101065 along with the previous detection of slow rotation in six other magnetic Ap stars indicates that there possibly exist other not yet identified slowly rotating Ap stars. Clearly, the detection and monitoring of such stars and the characterization of their stellar properties by future observations is extremely important for our understanding of their formation and the processes playing a role in achieving such super-slow rotation.

ACKNOWLEDGMENTS

The authors thank the anonymous referee for useful comments and C. R. Cowley for a valuable discussion. Based on observations made with ESO Telescopes at the La Silla Paranal Observatory under programme IDs 69.D-0210(A), 270.D-5023(A), 079.D-0240(A), 191.D-0255(I), 097.C-0277(A), and 099.C-0081(A). This work has made use of the VALD database, operated at Uppsala University, the Institute of Astronomy RAS in Moscow, and the University of Vienna.

REFERENCES

- Adelman S. J., 1981, *A&AS*, 44, 265
- Alecian E., Vilebrun F., Grunhut J., Hussain G., Neiner C., Wade G. A., 2017, arXiv:1705.10650
- Appenzeller I., Fricke K., Furtig W., et al., 1998, *The Messenger*, 94, 1
- Banerjee R., Pudritz R. E., 2006, *ApJ* 641, 949
- Braithwaite J., Nordlund A., 2006, *A&A*, 450, 1077
- Bychkov V. D., Bychkova L. V., Madej, J., 2016, *MNRAS*, 455, 2567
- Cauley P. W., Johns-Krull C. M., 2014, *ApJ* 797, 112
- Cowley C. R., Mathys G., 1998, *A&A*, 339, 165
- Cowley C. R., Ryabchikova T., Kupka F., Bord D. J., Mathys G., Bidelman W. P., 2000, *MNRAS*, 317, 299
- Cowley C. R., Hubrig, S., Ryabchikova T. A., Mathys G., Piskunov N., Mittermayer P., 2001, *A&A*, 367, 939
- Cowley C. R., Bidelman W. P., Hubrig S., Mathys G., Bord D. J., 2004, *A&A*, 419, 1087
- Donati J.-F., Semel M., Rees D. E., 1992, *A&A*, 265, 669
- Donati J.-F., Semel M., Carter B. D., Rees, D. E., Collier Cameron, A., 1997, *MNRAS*, 291, 658
- Elkin V. G., Kurtz D. W., Mathys G., Freyhammer L. M., 2010, *MNRAS*, 404, L104
- Elkin V. G., Kurtz D. W., Mathys G., 2015, *MNRAS*, 446, 4126
- Hubrig S., North P., Mathys G., 2000a, *ApJ*, 539, 352
- Hubrig S., North P., Medici A., 2000b, *A&A*, 359, 306
- Hubrig S., Cowley C. R., Bagnulo S., Mathys G., Ritter A., Wahlgren G. M., 2012, in *Exotic Stars as Challenges to Evolution*, ASP Conf. Proc., Vol. 279. Also IAU Colloquium 187. Edited by Christopher A. Tout and Walter Van Hamme. ISBN: 1-58381-122-2. San Francisco: Astronomical Society of the Pacific, p. 365
- Hubrig S., Szeifert T., Schöller M., Mathys G., Kurtz D. W., 2004a, *A&A*, 415, 685
- Hubrig S., Kurtz D. W., Bagnulo S., Szeifert T., Schöller M., Mathys G., Dziembowski W. A., 2004b, *A&A*, 415, 661
- Hubrig S., North P., Schöller M., 2007, *AN*, 328, 475
- Hubrig S., Ilyin I., Briquet M., Schöller M., Gonzalez J. F., Nunez N., De Cat P., Morel T., 2011, *A&A*, 531, L20
- Hubrig S., Schöller M., Ilyin I., Lo Curto G., 2013, *Astr. Nachr.*, 334, 1093
- Hubrig S., Carroll T. A. Schöller M., Ilyin I., 2015, *MNRAS* 449, L118
- Järvinen S. P., Hubrig S., Ilyin I., Schöller M., Briquet M., 2017, *MNRAS*, 464, L85
- Kudryavtsev D. O., Romanyuk I. I., Elkin V. G., Paunzen E., 2006, *MNRAS*, 372, 1804
- Kupka F., Dubernet, M.-L., VAMDC Collaboration, 2011, *Baltic Astr.*, 20, 503
- Kurtz D. W., Wegner G., 1979, *ApJ*, 232, 510
- Kurtz D. W., Elkin V. G., Mathys G., Riley J., Cunha M. S., Shibahashi H., Kambe E., 2004, *The A-Star Puzzle*, held in Poprad, Slovakia, July 8-13, 2004. Edited by J. Zverko, J. Ziznovsky, S. J. Adelman, and W. W. Weiss, IAU Symposium, No. 224. Cambridge, UK: Cambridge University Press, 2004., p. 343
- Kurtz D. W., Elkin V. G., Cunha M. S., Mathys G., Hubrig S., Wolff B., Savanov I., 2006, *MNRAS*, 372, 286
- Landolfi M., Landi Degl’Innocenti E., Landi Degl’Innocenti M., Leroy J. L., 1993, *A&A*, 272, 285
- Leroy J. L., Bagnulo S., Landolfi M., Landi Degl’Innocenti E., 1994, *A&A*, 284, 174
- Mathys G., 1989, *Fundamentals of Cosmic Physics*, 13, 143
- Mathys G., 1991, *A&AS*, 89, 121
- Mathys G., 1995, *A&A*, 293, 733
- Mathys G., Hubrig S., Landstreet J. D., Lanz T., Manfroid, J., 1997, *A&AS*, 123, 353
- Mathys G., Hubrig S., 2006, *A&A*, 463, 699
- Mathys G., 2015, *Physics and Evolution of Magnetic and Related Stars*, ASP Vol. 494, Proceedings of a conference held at the Special Astrophysical Observatory, Nizhny Arkhyz, Russia, 25-31 August 2014. Edited by Yu. Yu. Balega, I. I. Romanyuk, and D. O. Kudryavtsev
- Mathys G., 2017, *A&A*, 601, A14
- Metlova N. V., Bychkov V. D., Bychkova L. V., Madej J., 2014, *AstBu*, 69, 315
- Mashonkina L., Ryabchikova T., Ryabtsev A., 2005, *A&A*, 441, 309
- Mashonkina L., Ryabchikova T., Ryabtsev A., Kildiyarova R., 2009, *A&A*, 495, 297
- Mkrtychian D. E., Hatzes A. P., Kanaan, A., 2003, *MNRAS*, 345, 781
- Mkrtychian D. E., Hatzes A. P., Saio H., Shobbrook R. R., 2008, *A&A*, 490, 1109
- Nesvacil N., Hubrig S., Jehin E., 2004, *A&A*, 422, L51
- Press W. H., Teukolsky S. A., Vetterling W. T., Flannery B. P., 1992, *Numerical recipes in C. The art of scientific computing* Przybylski A., 1961, *Nature*, 189, 739
- Romanyuk I. I., Semenko E. A., Kudryavtsev D. O., 2014, *AstBu*, 69, 427
- Romanyuk I. I., Kudryavtsev D. O., Semenko E. A., Yakunin I. A., 2015, *AstBu*, 70, 456
- Ryabchikova T., Nesvacil N., Weiss W. W., Kochukhov O., Stütz, Ch., 2004, *A&A*, 423, 705
- Shulyak D., Ryabchikova T., Mashonkina L., Kochukhov O., 2009, *A&A*, 499, 879
- Shulyak D., Ryabchikova T., Kildiyarova R., Kochukhov O., 2010, *A&A*, 520, A88
- Snik F., Jeffers S., Keller C., Piskunov N., Kochukhov O., Valenti J., Johns-Krull, C., 2008, *SPIE*, 7014, 00

Stibbs D. W. D., 1950, MNRAS, 110, 395
Wolff S.C., 1976, ApJ, 202, 127
Wolff S.C., Hagen W., 1976, PASP, 88, 119

This paper has been typeset from a $\text{\TeX}/\text{\LaTeX}$ file prepared by the author.